

# EXTRAGALACTIC SOURCE COUNTS IN THE *SPITZER* 24 MICRON BAND: WHAT DO WE EXPECT FROM ISOCAM 15 MICRON DATA AND MODELS?

C. GRUPPIONI<sup>(1)</sup>, F. POZZI<sup>(2)</sup>, C. LARI<sup>(3)</sup>, S. OLIVER<sup>(4)</sup> AND G. RODIGHIERO<sup>(5)</sup>

*Draft version November 7, 2018*

## ABSTRACT

The comparison between the new *Spitzer* data at 24  $\mu\text{m}$  and the previous ISOCAM data at 15  $\mu\text{m}$  is a key tool to understand galaxy properties and evolution in the infrared and to interpret the observed number counts, since the combination of *Spitzer* with the *Infrared Space Observatory* cosmological surveys provides for the first time the direct view of the universe in the infrared up to  $z \gtrsim 2$ . We present the prediction in the *Spitzer* 24  $\mu\text{m}$  band of a phenomenological model for galaxy evolution derived from the 15  $\mu\text{m}$  data. Without any “a posteriori” update, the model predictions seem to agree well with the recently published 24  $\mu\text{m}$  extragalactic source counts, suggesting that the peak in the 24  $\mu\text{m}$  counts is dominated by starburst galaxies like those detected by ISOCAM at 15  $\mu\text{m}$  but at higher redshifts ( $1 \lesssim z \lesssim 2$  instead of  $0.5 \lesssim z \lesssim 1.5$ ).

*Subject headings:* galaxies: evolution – galaxies: starburst – cosmology: observations – infrared: galaxies.

## 1. INTRODUCTION

Cosmological constraints on the evolution of galaxies have been recently investigated by studying the statistical properties of large samples. In particular, the combined analysis of extragalactic source counts and redshift distributions is generally used to calibrate the theoretical models as a function of time. The mid-infrared (MIR) and far-infrared (FIR) regions of the electromagnetic spectrum probe the population of actively star-forming galaxies obscured by dust. Extragalactic source counts from different surveys over a wide flux range obtained with the ISOCAM instrument on board of the *Infrared Space Observatory* (ISO) indicate that these sources have evolved rapidly, significantly faster than deduced from optical surveys (Elbaz et al. 1999; Gruppioni et al. 2002; Metcalfe et al. 2003; Rodighiero et al. 2004). These results are supported by the detection of a substantial cosmic infrared background (CIRB; Hauser & Dwek 2001), which is interpreted as the integrated emission from dust present in galaxies. The contribution of resolved ISOCAM sources accounts for  $\sim 60\text{--}70\%$  of the CIRB at MIR frequencies, the bulk of this background originating in discrete sources at  $z \lesssim 1.2$  (Franceschini et al. 2001; Elbaz et al. 2002).

The *Spitzer Space Telescope* is now providing new insights into the IR population contributing to the CIRB, in particular with the Multiband Imaging Photometer 24  $\mu\text{m}$  band, which is starting to detect a population of galaxies that may be IR-luminous galaxies at  $z \sim 1.5 - 3$  (i.e. high-redshift analogs of the faint 15  $\mu\text{m}$  galaxies

detected by ISOCAM; see Chary et al. 2004). Preliminary results from the 24  $\mu\text{m}$  extragalactic source counts (Marleau et al. 2004; Papovich et al. 2004), confirming the existence of the rapidly evolving dust-obscured population discovered by ISOCAM, raise the question on how to compare them with the previous ISOCAM counts at 15  $\mu\text{m}$ . Both 24 and 15  $\mu\text{m}$  bands are extremely sensitive to the presence of broad emission features at 6.2, 7.7, 8.6, 11.3 and 12.7  $\mu\text{m}$  in the spectra of galaxies, probably from polycyclic aromatic hydrocarbons (PAHs; Puget & Leger 1989). Since these features dominate the photometric output at some redshifts, the ratio between the *Spitzer* 24  $\mu\text{m}$  and the ISOCAM 15  $\mu\text{m}$  fluxes ( $S_{24\mu\text{m}}/S_{15\mu\text{m}}$ ) is strongly dependent on  $z$ . In figure 1 this ratio versus  $z$  is shown for the populations contributing to the MIR source counts (see next section for a discussion): starburst galaxies (M82 spectral energy distribution [SED]), normal galaxies (M51), type 1 active galactic nuclei (AGNs; SED from Elvis et al. 1994), and type 2 AGNs (Circinus). As clearly shown in the plot, the 15  $\mu\text{m}$  band is optimized for detecting  $0.5 \lesssim z \lesssim 1.5$  galaxies, while the 24  $\mu\text{m}$  band is favored for the detection of galaxies at  $z \gtrsim 1.5$ . Since the comparison between the source counts in the two bands is a powerful tool for understanding the evolutionary properties of the different galaxy populations contributing to the counts at different redshifts and flux levels, it is worthwhile performing a careful comparison.

In a recent paper on extragalactic source counts from the First Look Survey (FLS), Marleau et al. (2004) try to compare the 24  $\mu\text{m}$  source counts with the previous 15  $\mu\text{m}$  counts from different ISOCAM surveys, transformed to 24  $\mu\text{m}$ . However, the reported transformation appears to be overly simplistic, since the ISOCAM counts (plotted in figure 4 of Marleau et al. (2004)) have been converted to the *Spitzer* 24  $\mu\text{m}$  band by considering a single value for the  $S_{24\mu\text{m}}/S_{15\mu\text{m}}$  flux ratio for all flux densities. The value used by the authors ( $S_{24\mu\text{m}}/S_{15\mu\text{m}} = 1.2$ ) is a median value derived from typical luminous infrared galaxy/ultraluminous infrared galaxy SEDs at relatively high  $z$  (Chary & Elbaz 2001), which is ap-

<sup>(1)</sup> Istituto Nazionale di Astrofisica: Osservatorio Astronomico di Bologna, via Ranzani 1, I-40127 Bologna, Italy.  
 e-mail: carlotta.gruppioni@bo.astro.it

<sup>(2)</sup> Dipartimento di Astronomia, Università di Bologna, via Ranzani 1, I-40127 Bologna, Italy

<sup>(3)</sup> Istituto di Radioastronomia del CNR, via Gobetti 101, I-40129 Bologna, Italy

<sup>(4)</sup> Astronomy Centre, Department of Physics & Astronomy, University of Sussex, Brighton BN1 9QJ, UK

<sup>(5)</sup> Dipartimento di Astronomia, Università di Padova, vicolo dell'Osservatorio 2, I-35122 Padova, Italy

appropriate only for sources making up the peak of the counts. In fact, as shown in figure 1, if we consider the “starburst” template (M82), we obtain a local value for the flux ratio of  $\sim 2.5$ , while we reach a value of  $\sim 1.3$  only at  $z \sim 1$ . Therefore, only the contribution to the counts made by galaxies with  $z$  around 1 could be transformed to  $24 \mu\text{m}$  using a flux ratio similar to that considered by Marleau et al. (2004). In particular, the bright part of the European Large-Area *ISO* Survey (ELAIS) counts (Gruppioni et al. 2002), linking the *IRAS* counts to the deep ISOCAM counts, is dominated by nearby non-evolving normal galaxies (with ratios of  $\sim 1.7$ ) and by starburst galaxies and type 2 AGNs (with ratios of  $\sim 2.5$  and  $\sim 2.3$ , respectively), as shown by La Franca et al. (2004). Therefore, the use of a single ratio value of 1.2 produces a misleading result [especially at  $S_{24\mu\text{m}} > 1 \text{ mJy}$ : i.e.  $15 \mu\text{m}$  counts shifted downwards by a factor of  $(1.7/1.2)^{1.5} - (2.5/1.2)^{1.5} = 1.7 - 3.0$ ], suggesting an apparent inconsistency between the bright part of the source counts in the two bands.

Since at the moment there are no large areas with available data at both wavelengths, we can make use of a model fitting the observed  $15 \mu\text{m}$  source counts (Pozzi et al. 2004, I. Matute et al. 2005, in preparation) to transform the counts from one frequency to the other, thus allowing a direct comparison.

In this Letter we discuss the more realistic way to transform the model predictions and the observed data from the LW3 band of ISOCAM to the  $24 \mu\text{m}$  band of *Spitzer*, in order to compare the properties of the  $24 \mu\text{m}$  sources with those of the ISOCAM  $15 \mu\text{m}$  ones. The Letter is structured as follows: in section 2, we describe the evolutionary model fitting the  $15 \mu\text{m}$  observables; in section 3.1, we show the model predictions at  $24 \mu\text{m}$ ; in section 3.2, we discuss a method to transform the observed data points from  $15$  to  $24 \mu\text{m}$ ; in section 4, we present our conclusions.

Throughout this Letter we will assume  $H_0 = 75 \text{ km s}^{-1} \text{ Mpc}^{-1}$ ,  $\Omega_m = 0.3$  and  $\Omega_\Lambda = 0.7$ .

## 2. THE MODEL

The model is based on the first direct determination of the  $15 \mu\text{m}$  luminosity function (LF) of galaxies and AGNs, based on data from the ELAIS southern fields survey (Lari et al. 2001; La Franca et al. 2004, Rowan-Robinson et al. 2004). We assume that four main populations, evolving independently, contribute to the observed source counts: starburst and normal galaxies and type 1 and 2 AGN. A maximum likelihood analysis (Marshall et al. 1983) has been used to simultaneously fit both evolution rates and shape parameters of the different local LFs. Although AGN make up a non negligible fraction of the extragalactic source counts at  $15 \mu\text{m}$  (especially at high flux densities), galaxies are the dominant class in the MIR.

The LF determination for galaxies, described extensively in Pozzi et al. (2004), is based on a sample of about 150 galaxies in the redshift interval  $0.0 \leq z \leq 0.4$ , covering a large flux density range between *IRAS* and the deep ISOCAM surveys ( $0.5 \leq S_{15\mu\text{m}} \leq 50 \text{ mJy}$ ). The normal, non evolving, and the starburst, evolving, populations are separated using the new criterion based on the MIR to optical luminosity ratio ( $L_{15\mu\text{m}}/L_R$ ). We use the basic Silva et al. (1998) models to reproduce the SED

of our prototypical galaxies, assumed to be M82 for the starburst population and M51 for the normal one. The MIR region (between 3 and  $18 \mu\text{m}$ ) of the modeled spectra were replaced with ISOCAM circular variable filter observations (M82: Forster-Schreiber et al. 2003; M51: Roussel et al. 2001). Note that, for simplicity, we have used a single template SED for each population, instead of different SEDs for different infrared luminosity intervals. While the normal population is consistent with no evolution, for the starburst population a strong evolution is found both in luminosity [ $L(z) \propto (1+z)^{3.5}$  up to  $z \sim 1$ ] and in density [ $\rho(z) \propto (1+z)^{3.8}$  up to  $z \sim 1$ ]. The evolutionary parameters of our model have been tested by comparing the model predictions with all the available observables, like source counts at all flux density levels (from 0.1 to 300 mJy) and redshift distributions and LF at high  $z$ . The agreement between the model predictions and the observed data is remarkably good (see figure 2 for an example of how the model fits the observed number counts at  $15 \mu\text{m}$ ).

The LF determination for AGNs (both type 1 and 2), described in I. Matute et al. (2005, in preparation), is based on ELAIS data (27 type 1 AGNs and 25 type 2 AGNs) combined with the local *IRAS* sample at  $12 \mu\text{m}$  of Rush, Malkan & Spinoglio (1993), converted to  $15 \mu\text{m}$  using appropriate SEDs (41 type 1 AGNs and 50 type 2 AGNs). The typical SED assumed for type 1 AGNs is that compiled by Elvis et al. (1994), while for type 2 AGN two extreme cases of the obscured AGN SED in the MIR were assumed: a starburst-like SED (Circinus; Sturm et al. 2000) and an AGN-like SED (NGC 1068; Sturm et al. 2000). Type 1 AGNs are found to evolve with a luminosity evolution [ $L(z) \propto (1+z)^{k_L}$ ], with an evolution rate  $k_L$  equal to 2.6 up to  $z \sim 2$  and constant thereon. A similar evolutionary scenario is found for type 2 AGNs, with  $k_L$  ranging from 2.0 to 2.6 depending on the adopted SED (NGC 1068 or Circinus, respectively). The best-fitting model is found to reproduce well both observed source counts and redshift distributions, as shown by I. Matute et al. (2005, in preparation).

## 3. COUNTS AT 24 MICRON

### 3.1. Model Predictions at $24 \mu\text{m}$

By using the appropriate SED for each population and convolving the SED with the appropriate filter transmission, the galaxy and AGN local LFs have been transformed from  $15$  to  $24 \mu\text{m}$ . Then the predicted  $24 \mu\text{m}$  source counts have been computed for all the contributing populations. In figure 3, the source counts predicted by our model are compared to the recently published *Spitzer*  $24 \mu\text{m}$  data from the FLS (Marleau et al. 2004), from the deep surveys (Papovich et al. 2004) and from the *Spitzer* Wide-Area Infra-red Extragalactic Survey (SWIRE; D.L. Shupe et al. 2005, in preparation). We can notice a consistency between data and model, with no need, at least in first approximation, for the use of more extreme SEDs for starburst galaxies (i.e., Arp 220). AGNs (either type 1 or 2) do not dominate the observed source counts at any flux level, although type 2 make about 25% of the counts at  $S_{24\mu\text{m}} > 10 \text{ mJy}$ . The counts are dominated by non evolving normal galaxies at  $\gtrsim 8 \text{ mJy}$  and by evolving starburst galaxies at lower flux densities. The assumption made in our model of no evo-

lution for galaxies at  $z > 1$ , not very well constrained by ISOCAM data, is “a posteriori” consistent with *Spitzer* data.

It is interesting to see how the ratio between the *Spitzer* 24 and the ISOCAM 15  $\mu$ m flux for all the populations changes as a function of  $z$  (figure 1) and of the 24  $\mu$ m flux (as derived by our model; figure 4). The comparison between figs 1 and 4 clearly shows that the higher flux densities ( $S_{24\mu\text{m}} > 2 - 3$  mJy) are dominated by nearby objects with moderately high values of the  $S_{24\mu\text{m}}/S_{15\mu\text{m}}$  ratio ( $\sim 2.2$ : starburst and type 2 AGNs;  $\sim 1.7$ : normal galaxies), while the bump of the 24  $\mu$ m counts (at fluxes 0.1 – 1 mJy) is dominated by objects with  $S_{24\mu\text{m}}/S_{15\mu\text{m}} \approx 1.4$  (mainly starburst galaxies at  $0.7 \lesssim z \lesssim 1.5$ ). These are the same populations found to contribute to the ISOCAM 15  $\mu$ m source counts. However, since we have approximately

$$\left(\frac{dN}{dS} S^{2.5}\right)_{24\mu\text{m}} = \left(\frac{dN}{dS} S^{2.5}\right)_{15\mu\text{m}} \left(\frac{S_{24\mu\text{m}}}{S_{15\mu\text{m}}}\right)^{1.5}. \quad (1)$$

and the ratio value at flux densities around the peak of the differential source counts is  $\simeq 1.4$ , the evolutionary excess is more pronounced at 15  $\mu$ m than at 24  $\mu$ m. At the lower flux densities ( $S_{24\mu\text{m}} \lesssim 0.1$  mJy), sources with high flux ratio values ( $S_{24\mu\text{m}}/S_{15\mu\text{m}} > 2.0 - 2.5$ , corresponding to  $z > 1.5$ ) start to dominate the counts. These high- $z$  starburst galaxies, mainly at  $1.5 \leq z \leq 2.5$ , are not visible in the ISOCAM surveys, because of the 15  $\mu$ m  $k$ -correction, but contribute to the fainter end of the 24  $\mu$ m source counts and to the 24  $\mu$ m cosmic background. Since the existence of this starburst population at high redshift is predicted just by extrapolating our 15  $\mu$ m model to higher  $z$ , it is likely that faint 24  $\mu$ m sources are the high-redshift likes of the fainter 15  $\mu$ m sources detected by ISOCAM (see also Chary et al. 2004).

The same kind of considerations are evident from figure 5, where the contributions to the 24  $\mu$ m number counts from different redshift intervals are shown. While galaxies with  $0.0 \lesssim z \lesssim 0.5$  dominate the high fluxes ( $S_{24\mu\text{m}} \gtrsim 2$  mJy), the peak of the differential counts is made mainly by  $0.5 \lesssim z \lesssim 1.5$  sources, although at  $S_{24\mu\text{m}} \lesssim 0.16$  mJy (corresponding roughly to the limit of the deepest, non-lensed, ISOCAM survey:  $S_{15\mu\text{m}} = 0.12$  mJy; see figure 5) the higher- $z$  population contributes for a conspicuous fraction ( $\sim 46\%$ ). By extrapolating the source counts model down to the faintest fluxes, we obtain an estimate of the total 24  $\mu$ m background:  $\nu I_\nu(24\mu\text{m}) \sim 2.4$  nWm $^{-2}$ sr $^{-1}$ . According to our model, the amount produced by sources at  $z \lesssim 1.5$  is  $\sim 1.6$  nWm $^{-2}$ sr $^{-1}$ , therefore  $\sim 66\%$  of the 24  $\mu$ m background originates at relatively low redshift. From the comparison between the total background predicted by our model and the value derived from the observed 24  $\mu$ m source counts ( $1.9 \pm 0.6$  nW m $^{-2}$  sr $^{-1}$ ; Papovich et al. 2004), we find that the *Spitzer* deep surveys already resolve  $\sim 78\%$  of the total 24  $\mu$ m background.

### 3.2. Observed ISOCAM Counts Transformed to 24 $\mu$ m

To compare observed data counts at 15  $\mu$ m with those at 24  $\mu$ m, we have converted the 15  $\mu$ m source counts obtained from different ISOCAM surveys (from the ultra-deep lensed of Metcalfe et al. 2003, to the shallower ELAIS Survey of Gruppioni et al. 2002) to 24

$\mu$ m, as described in the following text. We have convolved the observed 15  $\mu$ m differential counts ( $\frac{dN}{dS_{15\mu\text{m}}}$ ) with the distribution of the ratios  $S_{24\mu\text{m}}/S_{15\mu\text{m}}$  obtained from our model, given a 15  $\mu$ m source selection ( $f[(S_{24\mu\text{m}}/S_{15\mu\text{m}}), S_{15\mu\text{m}}]$ ):

$$dN(S_{24\mu\text{m}}) = \int f\left(\frac{S_{24\mu\text{m}}}{S_{15\mu\text{m}}}, S_{15\mu\text{m}}\right) \frac{dN}{dS_{15\mu\text{m}}}(S_{15\mu\text{m}}) dS_{15\mu\text{m}} \quad (2)$$

Data at 15  $\mu$ m from different samples have been combined by weighting each point by its formal error (inverse of the squared error). In figure 3 the counts derived from the 15  $\mu$ m observed data (shaded area) are overplotted to the 24  $\mu$ m data and model. The two different source counts are consistent and, in first approximation, seem to agree well. In particular, at high flux densities we do not observe the discrepancy as reported by Marleau et al. (2004), thanks to a more accurate flux density ratio applied. On the other hand, the discrepancy observed at 24  $\mu$ m fluxes lower than  $\sim 0.05$  mJy is only apparent, since fluxes fainter than this are not sampled by the 15  $\mu$ m data. Some level of inconsistency between the two source counts are visible around  $\sim 1$  mJy, where the 15  $\mu$ m counts (and the model) are higher than the observed 24  $\mu$ m source counts. A decrease of the  $S_{24\mu\text{m}}/S_{15\mu\text{m}}$  ratio around 1 mJy could be obtained by slightly modifying the starburst template in the MIR range (i.e. increasing the PAH features with respect to the continuum, since at the typical redshift of sources with these flux densities,  $z \approx 1$ , the PAH features enter the 15  $\mu$ m band). A similar change was made by Lagache et al. (2004), who show how a minor change in the starburst template spectra between 12 and 30  $\mu$ m (together with a slight modification of the luminosity density) was a sufficient a posteriori modification to enable a model not fitting the observed 24  $\mu$ m source counts (Lagache et al. 2003) to reproduce the observations.

We are actually working at improving the model–data agreement by including also the recently published 24  $\mu$ m source counts (and all the MIR–FIR counts and redshift distributions available in literature) as an observational constraint to the maximum likelihood analysis of our 15  $\mu$ m-based model. Moreover, we are considering the use of an SED library, with different SEDs associated not only to different populations, but also to different luminosity classes (i.e. Chary & Elbaz 2001). The model improvements will be described in a future paper (F. Pozzi et al. 2005, in preparation), since they are beyond the scope of the present Letter, whose intent is just to show, through a simple 15  $\mu$ m-based model, what the 24  $\mu$ m/15  $\mu$ m comparison can tell us in terms of galaxy evolutionary properties.

## 4. CONCLUSIONS

We have discussed the importance of a comparison between the extragalactic source counts in two different MIR bands for the study of the evolutionary properties of galaxies. We have shown what we expect in terms of variations of the  $S_{24\mu\text{m}}/S_{15\mu\text{m}}$  flux density ratio with redshift and 24  $\mu$ m flux, considering typical SEDs for the different populations contributing to the source counts. Then, to compare the observed *Spitzer* 24  $\mu$ m source counts with the ISOCAM 15  $\mu$ m ones, we have presented the prediction in the 24  $\mu$ m *Spitzer* band from a phenomenological

evolution model based on the ISOCAM 15  $\mu\text{m}$  LF of galaxies and AGNs. Actually, this model is the only one available in literature that is able to reproduce the observed 24  $\mu\text{m}$  source counts without the need, at least in first approximation, of any a posteriori updates. We have also shown that the observed ISOCAM data points transformed from 15  $\mu\text{m}$  to 24  $\mu\text{m}$  seem to agree well with the recently published *Spitzer* source counts. Our model suggests the appearance of a new population of

high redshift ( $z > 1.5$ ) galaxies at 24  $\mu\text{m}$ , not detected in the previous ISOCAM surveys, but probably the high- $z$  likes of the 15  $\mu\text{m}$  sources.

We thank the anonymous referee for valuable comments that improved the quality of this Letter and D.L. Shupe and I. Matute for kindly providing SWIRE data counts and AGN models before publication.

#### REFERENCES

- Chary, R., & Elbaz, D. 2001, *ApJ*, 556, 562  
 Chary, R., et al. 2004, *ApJS*, 154, 80  
 Elbaz, D., et al. 1999, *A&A*, 351, L37  
 Elbaz, D., et al. 2002, *A&A*, 384, 848  
 Elvis, M., et al. 1994, *ApJS*, 95, 1  
 Förster Schreiber, N.M., et al. 2003, *A&A*, 399, 833  
 Franceschini, A., et al. 2001, *A&A*, 378, 1  
 Gruppioni, C., et al. 2002, *MNRAS*, 335, 831  
 Hauser, M.G. & Dwek, E. 2001, *ARA&A*, 39, 249  
 La Franca, F., et al. 2004, *AJ*, 127, 3075  
 Lagache, G., Dole, H., & Puget, J.-L. 2003, *MNRAS*, 338, 555  
 Lagache, G., et al. 2004, *ApJS*, 154, 112  
 Lari, C., et al. 2001, *MNRAS*, 325, 1173  
 Marleau, F., et al. 2004, *ApJS*, 154, 66  
 Marshall, H.L., et al. 1983, *ApJ*, 269, 35  
 Metcalfe, L., et al. 2003, *A&A*, 407, 791  
 Papovich, C., et al. 2004, *ApJS*, 154, 70  
 Pozzi, F., et al. 2004, *ApJ*, 609, 122  
 Rodighiero, G., et al. 2004, *A&A*, 427, 773  
 Roussel, H., et al. 2001, *A&A*, 369, 473  
 Rowan-Robinson, M., et al. 2004, *MNRAS*, 351, 1290  
 Rush, B., Malkan, M.A. & Spinoglio L. 1993, *ApJS*, 89, 1  
 Silva, L., et al. 1998, *ApJ*, 509, 103

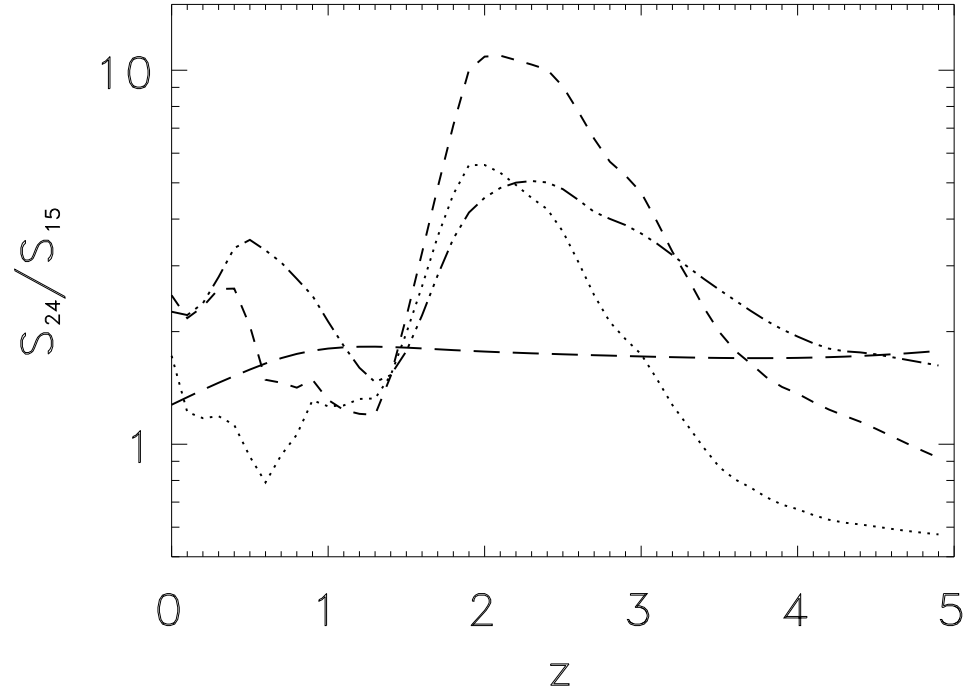


FIG. 1.—  $S_{24\mu m}/S_{15\mu m}$  ratio as a function of redshift for the MIR populations contributing to the observed number counts: starburst galaxies (short-dashed line: M82 SED prototype), normal galaxies (dotted line: M51), type 2 AGN (dot-dot-dot-dashed line: Circinus) and type 1 AGN (long-dashed line: SED from Elvis et al. 1994).

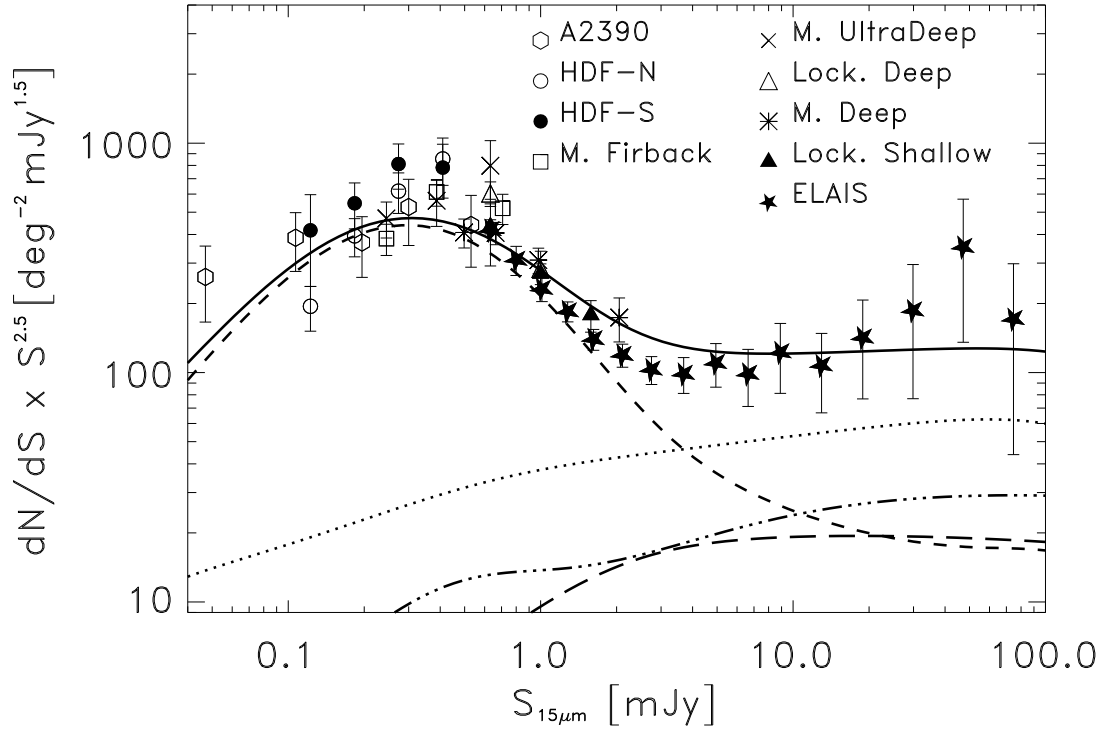


FIG. 2.— Normalised differential source counts in the ISOCAM  $15\ \mu\text{m}$  band. As explained in the plot, data points are from several surveys (HDF-N, HDF-S, Marano Firback, Ultra-Deep and Deep: Elbaz et al. 1999b; Ultra-Deep lensed: Metcalfe et al. 2003; ELAIS-S1: Gruppioni et al. 2002; Lockman Deep and Shallow: Rodighiero et al. 04). The model curves are from Pozzi et al. (2004) for galaxies (dash: starburst; dot: normal) and from Matute et al. (in preparation) for AGN (long-dash: type 1; dot-dot-dot-dash: type 2).

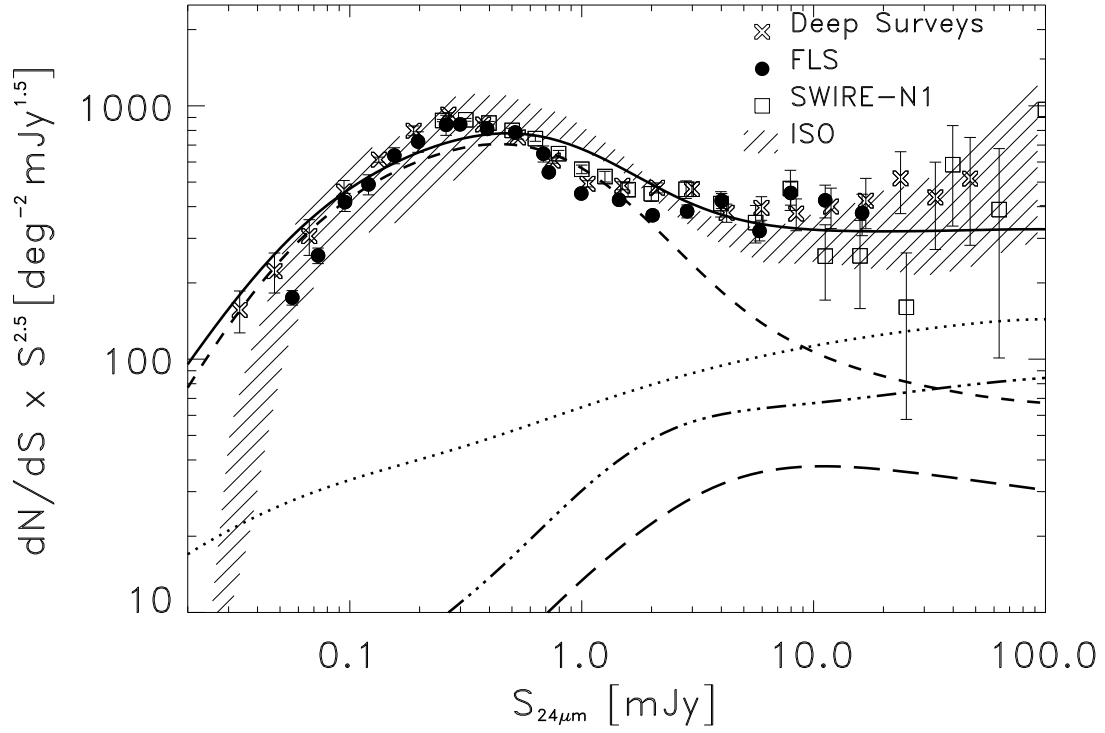


FIG. 3.— Normalised differential source counts at 24  $\mu$ m (crosses: Deep *Spitzer* Surveys, Papovich et al. 2004; filled circles: FLS, Marleau et al. 2004; open squares: SWIRE-N1, Shupe et al. in prep.) with the model predictions (as in figure 2) and the 15  $\mu$ m data (shaded region) transformed to 24  $\mu$ m as described in the text.

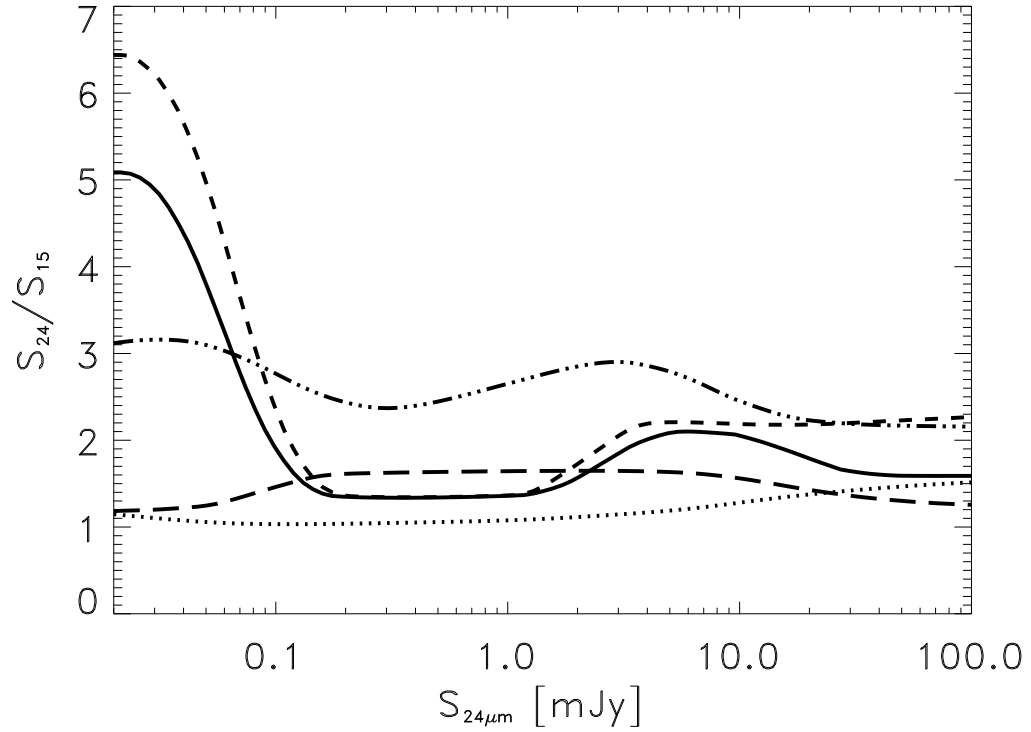


FIG. 4.— Median values of the  $S_{24\mu\text{m}}/S_{15\mu\text{m}}$  flux density ratio as function of  $S_{24\mu\text{m}}$ , as derived by our model for all the populations (weighted mean: solid line; different populations: lines as in previous figures).

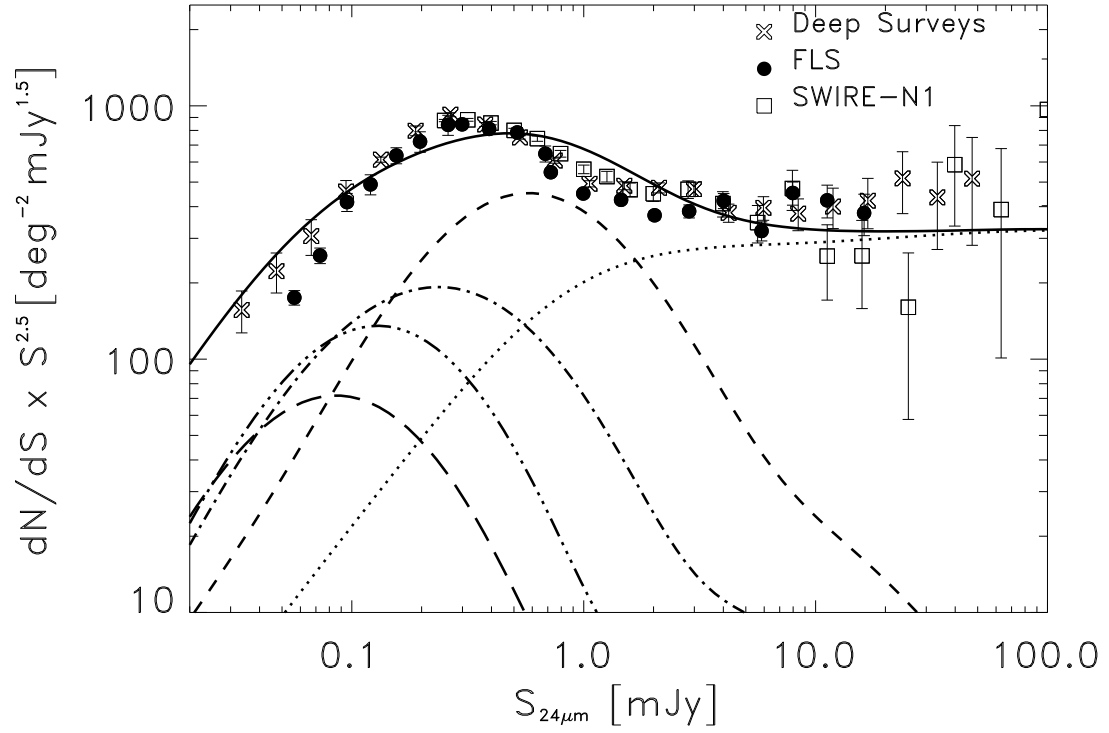


FIG. 5.— Differential redshift contribution to the normalized differential source counts at 24  $\mu\text{m}$ . The dotted, dashed, dot-dashed, dot-dot-dot-dashed and long-dashed lines correspond to the 0.0–0.5, 0.5–1.0, 1.0–1.5, 1.5–2.0 and 2.0–2.5 redshift intervals respectively.